Smectic C Structure and Backbone Confinement in Side-on Fixed Liquid Crystalline Polymers

S. Lecommandoux,*,† L. Noirez,‡ M. F. Achard,§ and F. Hardouin§

Laboratoire de Chimie des polymères Organiques, Université Bordeaux 1, ENSCPB, BP108, Av. Pey Berland, 33402 Talence Cedex 2, France, Laboratoire Léon Brillouin (CEA-CNRS), CE-Saclay, 91191 Gif-sur-Yvette, France, and Centre de Recherche Paul Pascal, Université Bordeaux 1, Av. A. Schweitzer, 33600 Pessac, France

Received July 9, 1999; Revised Manuscript Received October 28, 1999

ABSTRACT: The influence of the rate of dilution of the mesogens along the polymer backbone on the conformation and the structure of two different side-on mesogens polysiloxanes are studied using neutron-scattering techniques. The average backbone conformation in the nematic and smectic C phases is deduced from small-angle neutron-scattering measurements. An inversion in the backbone conformation from prolate in the nematic phase to highly oblate in the smectic phase is evidenced. Distribution profiles of polysiloxane main chains are calculated from neutron diffraction experiments in the smectic phase. A transition in the confinement of the main chain within the layers has been demonstrated: the polymer backbone can be segregated between the layers, but also present in the middle part of the mesogenic layers.

I. Introduction

Side-on fixed liquid crystal polymers (LCPs) represent a peculiar class of side chain LCPs in which the mesogenic group is laterally attached to the polymer backbone. This kind of molecular architecture gives rise preferentially to the nematic phase,[1] but also, more recently evidenced to smectic phases.[2] The smectic phase is based on the association in layer of the mesogenic parts. In the case of usual side-chain liquid crystal polymers (SCLCPs), it was first admitted,[3] then hinted by X-ray,[4a−c] finally demonstrated by neutron diffraction[4d] that the polymer backbones are mostly segregated between the mesogenic layers. However, the profile of backbone repartition is rarely a simple function, and it even appears that, in certain cases, the polymer backbones partially fill the middle zone of the mesogenic layers.[10]

Specifically, considering the situation of side-on fixed LCPs, we have recently shown the occurrence of a strong oblate anisotropy of the backbone conformation in the smectic C phase[6] with respect to the normal of the layers, as in the case of a smectic A phase of a side-end fixed LCP.[7] However, since of the attachment site of the spacer, the internal arrangement within the layer of side-on fixed mesogens remains unknown compared to usual side-end polymer. Moreover, by decreasing the temperature from the nematic phase down to the smectic C phase, an original inversion of the backbone conformation is observed which changes from prolate to oblate[6] and should be associated with strong internal reorganizations. In addition, this side-on fixed LCP displays also an original behavior in the thermodynamical and structural properties by changing the mesogenic ratio per chain (dilution):[8] the presence of a maximum of nematic to smectic C enthalpy ΔH_{NSc} (and entropy ΔS_{NSc}) is associated with a given "dilution" X_{opt} for which the Sc tilt angle is a minimum.

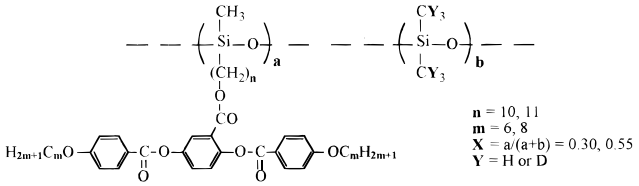

Figure 1. General chemical formula of the side-on fixed LCPs under study. Dilution $X = a/(a + b) = 0.30, 0.55$; $n = 10, 11$; $m = 6,8$; Y = H (hydrogenated), D (deuterated).

In this paper, we aim at studying on one hand the backbone conformation before and after this "dilution" X_{opt}, using small-angle neutron scattering (SANS) on specifically deuterated polymers, and on the other hand the localization of the backbone chains within the layers corresponding to each dilution by a combination of different neutron diffraction patterns.

II. Experimental Section

The thermodynamical and structural properties of these polysiloxanes have been already exposed in a previous paper.[6,8] They correspond to the chemical formula presented in Figure 1. Two different mesogens are studied. The first one is obtained with a spacer $n = 10$ and aliphatic tails $m = 6$ and a second one with $n = 11$ and $m = 8$. For each of them, two dilution rates have been tested by fixing mesogenic groups to a polysiloxane backbone via hydrosylilation with a ratio of 55% and 30%. The equivalent liquid crystalline polymers hydrogenated and deuterated on the backbone have been synthesized (Y=H or D).

The transition temperatures T, transition entropies ΔS, wave vector **q**, tilt angle θ, degree of polymerization in number $\overline{DP_n}$, and polymolecular index I are given in Table 1 for each compound. The number-average molecular weight of each compound (Y = H or D) has been determined by size exclusion chromatography using a self-made polysiloxane standardization. This last one has been carried out using tonometry measurements of polysiloxane standards. Similar values were

* Author for correspondence. Telephone: (33) 5 57 96 22 41. Fax: (33) 5 56 84 84 87. E-mail: lecomman@enscpb.u-bordeaux.fr.
† Laboratoire de Chimie des polymères Organiques, Université Bordeaux 1.
‡ CE-Saclay.
§ Centre de Recherche Paul Pascal, Université Bordeaux 1.

10.1021/ma9911086 CCC: $19.00
Published on Web 12/11/1999

Table 1. Transition Temperature (°C), Transition Entropies ΔS_{IN} and ΔS_{NSc} (J·μm^{-2}·K^{-1}), Wave Vector q (Å^{-1}), Tilt Angle θ (deg), Degree of Polymerization in Number $\overline{DP}_n$ and Polymolecular Index I for the Hydrogenated (H) or Deuterated (D) Polymers $P_{10,6,6}$ 30% and 55% and $P_{11,8,8}$ 30% and 55%

polymer	Y	transition temp g−Sc−N−I	ΔS_{NSc}	ΔS_{IN}	$\overline{DP}_n$	I	q	θ
$P_{10,6,6}$ 30%	H	10−61−72	3.0	0.4	90	1.2	0.195	47
	D	10−62−71	3.0	0.4	70	1.2	0.195	47
[a]$P_{10,6,6}$ 55%	H	14−49−76	1.9	0.85	55	1.2	0.21	44
	D	14−49−71	1.9	0.8	55	1.2	0.21	44
$P_{11,8,8}$ 30%	H	2−70−75	3.3	0.5	90	1.2	0.185	42
	D	2−70−75	3.3	0.5	70	1.2	0.185	42
$P_{11,8,8}$ 55%	H	8−70−83	3.9	1.0	55	1.2	0.21	46
	D	9−70−84	3.9	1.0	55	1.2	0.21	46

[a] According to ref 6.

found for the hydrogenated and the deuterated polymers. The transition temperatures, thermodynamic parameters, and structural characteristics were also found to be the same for both hydrogenated and deuterated polymers. The H/D blends necessary to the SANS and ND experiments can be used to determine coherent values of the radii of gyration and diffraction intensity without taking into account the effect of molecular weight and mass distribution.

Disklike cells (15 mm diameter, 1 mm thickness) were prepared for the hydrogenated polymer and the mixture (H + D) of each compound. The orientation of the samples for the SANS experiments was obtained by decreasing slowly the temperature from the isotropic phase down to the room temperature under an external magnetic field of 1.4 T. The neutron equipment used was the two-dimensional multidetector PAXY of the Léon Brillouin Laboratory.

The polymer dimensions were obtained at small angles with a multidetector-sample distance of 2 m and a wavelength of 10 Å (7×10^{-3} Å$^{-1} < q < 7 \times 10^{-2}$ Å^{-1}). A linear dependence of the inverse of the scattered intensity $I^{-1}(q)$ versus q^2 is observed over this q range. Since both polymers (H and D) display equivalent molecular weights, the intensity can be modeled following the Zimm representation in the Guinier domain:

$$I^{-1}(q_{||}) = I^{-1}(0)(1 + q_{||}^2 R_{||}^2)$$

$$I^{-1}(q_{\perp}) = I^{-1}(0)(1 + q_{\perp}^2 R_{\perp}^2)$$

where q_i is the component of the scattered vector in the direction parallel or perpendicular to the magnetic field (i = || or ⊥), and R_i represents the quadratic size of the labeled polymers in the direction i. The temperature dependence of these dimensions could also be reported with an error estimated to be less than 5%.

The neutron diffraction experiments were made with a multidetector−sample distance of 2 m and a wavelength of 4 Å in order to gain access to larger angles. Only two smectic reflections (001 and 002) are detected. Because of the inherent difficulty to evaluate the orientation quality of a smectic C phase aligned via a magnetic field and since of the necessity of obtaining an optimal alignment for each sample (the profiles are subtracted), the measurements were finally carried out on unoriented samples (powder). So, a similar orientation quality was ensured. The procedure adopted to determine the distribution profile of the main chains in the smectic layers is based on the following assumptions.[5,9] As for SANS measurements, the determination of the 001 and the 002 smectic reflection intensities have been done on normalized data corrected from the background noise (incoherent scattering, electronic noise...). The intensities are reported to the same number of scatterers (the cells contain the same quantity of polymer) and corrected from the Lorentz factor. Since the smectic phase is a continuous periodic function, it can be described by a Fourier series expanded with cosine terms:

$$\rho(z) = \rho_0 + \sum_i A_i \cos\frac{2\pi z}{d} i$$

with d as the layer spacing and $\rho(z)$ as the density of coherent scattering along the director.

The scattering function associated with this modulation is obtained via the Fourier transform. The intensity of each smectic reflection is then assimilated to the square of each amplitude term A_i:

$$S(q_z) \alpha \sum_i A_i^2 \delta\left(q_z - \frac{2\pi i}{d}\right)$$

Once $|A_i|$ is known, the determination of the profile of coherent scattering is then reduced to the determination of the sign of each A_i coefficient. Every possible combination of sign is examined, and assuming that the layers are filled by the mesogens and that the deuteration site provides a positive contribution to the profile, only one physically acceptable combination is kept. Then, the profile of the main-chain distribution is deduced from the subtraction of the function corresponding to the H/D mixture

$$\Delta\rho(\text{H/D}) = \rho(\text{H/D}) - \rho_0 = A_1(\text{H/D}) \cos\frac{2\pi z}{d} + A_2(\text{H/D}) \cos\frac{4\pi z}{d} \quad (1)$$

from the function corresponding to the fully hydrogenated polymer:

$$\Delta\rho(\text{H}) = \rho(\text{H}) - \rho_0 = A_1(\text{H}) \cos\frac{2\pi z}{d} + A_2(\text{H}) \cos\frac{4\pi z}{d} \quad (2)$$

III. Results and Discussion

III.1. Determination of the Polymer Conformation. Figure 2 displays the evolution of the polymer dimensions $R_{||}$ and $R_{\perp}$ as a function of the temperature for the $P_{10,6,6}$ 55% (Figure 2a), $P_{10,6,6}$ 30% (Figure 2b), $P_{11,8,8}$ 55% (Figure 2c), and $P_{11,8,8}$ 30% (Figure 2d). The results for the $P_{10,6,6}$ 55% are published in ref 6.

We can observe at high temperature a same evolution for each compound with a weak prolate anisotropy of the backbone conformation characterizing the nematic phase ($R_{||}/R_{\perp} = 1.2$) and an inversion of the conformation to an oblate shape in the smectic C phase. We can insist on the fact that this kind of inversion of the backbone conformation is very original: it is the first inversion from prolate in the nematic phase to oblate in the low-temperature smectic C phase. Moreover, we can demonstrate that, as we have described for the $P_{10,6,6}$ 55%, this inversion is reversible, and the layers of the smectic C arrangement are perpendicular to the average magnetic field direction. The anisotropic ratios ($R_{||}/R_{\perp}$) in the nematic and smectic C phases are summarized in Table 2 for each sample.

By decreasing the "dilution" from 55% to 30% of the mesogen/repetitive units, we can observe a decrease in the nematic phase of the prolate anisotropy of the backbone. In contrast, in the smectic C phase, the increase of the "dilution" induces a stronger oblate anisotropy. This can reveal a more important confinement of the polymer main chains. The question of the dependence of the backbone confinement with the smectic order parameter and with the type of the smectic structure[10] is raised here. This question will be discussed in part III.2 from the determination of the distribution profiles of the main chains in the smectic C phase.

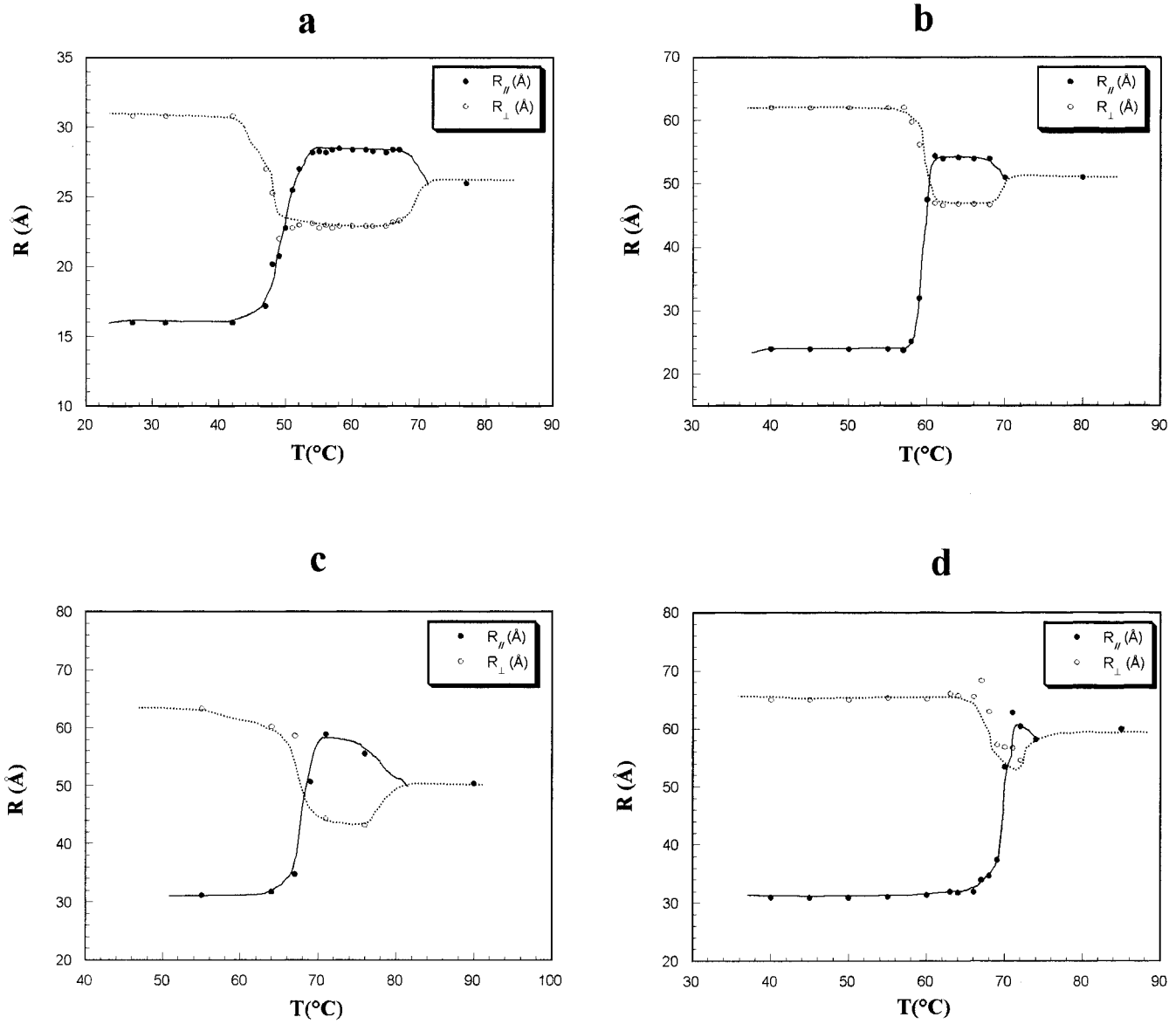

Figure 2. Values of the backbone dimensions respectively parallel and perpendicular to the magnetic field direction $R_{||}$ (●)and $R_{\perp}$ (○) as a function of the temperature for $P_{10,6,6}$ 55% (a), $P_{10,6,6}$ 30% (b), $P_{11,8,8}$ 55% (c), and $P_{11,8,8}$ 30% (d). Data for part a are reported according to ref 6.

Table 2. Saturated Values of the Anisotropy Ratio ($R_{||}/R_{\perp}$) in the Nematic (N) and Smectic C (Sc) Phases for the Polymers under Study

polymer	$R_{||}/R_{\perp}$ (N)	$R_{||}/R_{\perp}$ (Sc)
[a] $P_{10,6,6}$ 55%	1.2	0.5
$P_{10,6,6}$ 30%	1.1	0.4
$P_{11,8,8}$ 55%	1.3	0.6
$P_{11,8,8}$ 30%	1.1	0.5

[a] Results from ref 6.

Considering the nematic phase, it is well-known for side-end fixed LCPs that the type and rate of the anisotropy of the polymer backbone depends on the presence or not of smectic fluctuations.[11] In the case of a nematic−smectic A transition, the anisotropy of the backbone is slightly oblate in the nematic phase: it is interpreted threw the existence of smectic A fluctuations in the nematic phase. The present situation differs from the side-end polymers. First, we observed a prolate backbone shape in the nematic phase. Moreover, we have evidenced by neutron diffraction the occurrence of smectic C fluctuations (cybotactic groups) in the nematic phase for the dilution 55% ($P_{10,6,6}$ 55% and $P_{11,8,8}$ 55%) and not for the dilution 30% ($P_{10,6,6}$ 30% and $P_{11,8,8}$ 30%). Thus, we can conclude in that case that the smectic fluctuations do not seem to be the relevant parameter for the backbone conformation in the nematic phase: as opposed to side-end LCPs, the backbone conformation in side-on LCPs is not directly related to the presence of the Sc fluctuations.

Figure 3 shows the evolution of the radii of gyration R_g ($R_g^2 = R_{||}^2 + 2R_{\perp}^2$) as a function of the temperature for the four compounds under study.

The radii of gyration follow the same evolution for all of them. From isotropic to nematic phase, R_g decreases, and increases from nematic to smectic C phase. The evolution of the global radius of gyration is interesting. The reduction of R_g through the I−N transition is associated with a loss of excluded volume once the mesogens are oriented along one direction in the nematic phase. However, the decoupling between the backbone and the mesogens is efficient since the prolate

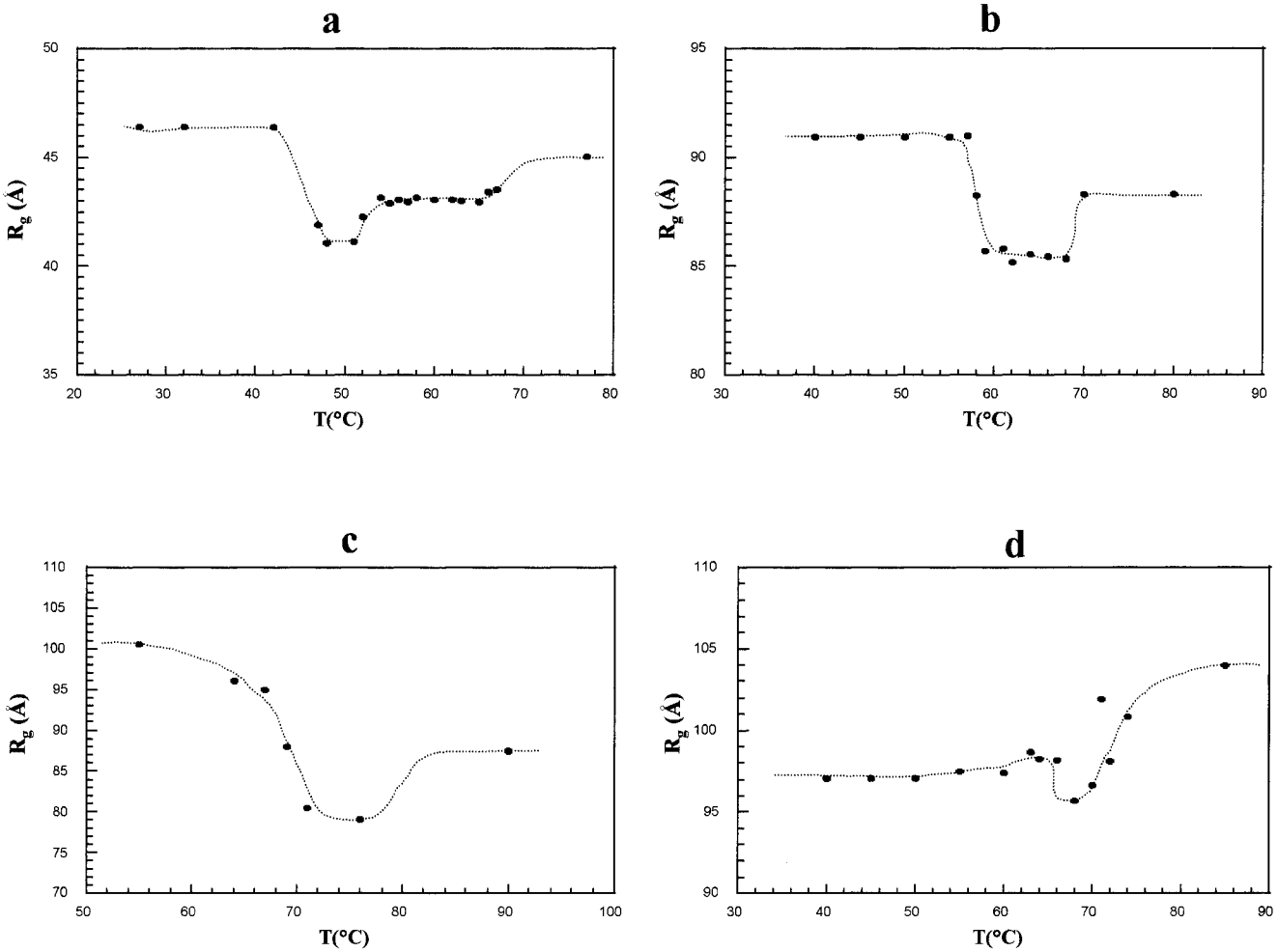

Figure 3. Evolution of the backbone radii of gyration R_g ($R_g^2 = R_{||}^2 + 2R_{\perp}^2$) as a function of the temperature for $P_{10,6,6}$ 55% (a), $P_{10,6,6}$ 30% (b), $P_{11,8,8}$ 55% (c), and $P_{11,8,8}$ 30% (d).

anisotropy remains small. This is no longer the case in the smectic phase, and the N−Sc transition is associated with a significant increase of R_g. This increase has to be interpreted by a rigidification of the polymer backbone and thus a loss of decoupling spacer/mesogen. It involves a direct participation of the spacer to the layer (Figure 5) together probably with an extension of the nonmesogenic backbone part. So, the liquid crystalline field does not only favor the backbone orientation, but even acts on the statistics of the backbone (i.e., rigidification).

III.2. Determination of the Main-Chain Profile. The determination of the profile of the polysiloxane backbone is deduced from the subtraction of eq 1 to eq 2. As a result, we obtained the following profiles:

for $P_{10,6,6}$ $\rho(P_{10,6,6}\ 55\%) = 1.447 \cos\frac{2\pi z}{30} + \cos\frac{4\pi z}{30}$ with a layer distance of 30 Å

$\rho(P_{10,6,6}\ 30\%) = 1.65 \cos\frac{2\pi z}{32} + 1.55 \cos\frac{4\pi z}{32}$ with a layer distance of 32 Å

for $P_{10,8,8}$

$\rho(P_{11,8,8}\ 55\%) = 2.21 \cos\frac{2\pi z}{30} + 1.385 \cos\frac{4\pi z}{30}$ with a layer distance of 30 Å

$\rho(P_{11,8,8}\ 30\%) = 1.55 \cos\frac{2\pi z}{34} + 0.95 \cos\frac{4\pi z}{34}$ with a layer distance of 34 Å

The profiles obtained are represented in Figure 4 for all the compounds as a function of the layer thickness.

The excess of density on each side of the diagram corresponds to the main chains confined between the layers. Nevertheless, a bump appears systematically in the middle of the mesogenic layers, which should be interpreted as the presence of the backbones in this central part. Moreover, the bump is small for the polymers with 55% of mesogens, and becomes pretty large for the ones with 30% of mesogens. As detailed elsewhere, the presence of this bump is essentially due to the strong 002 reflection observed in the H/D mixtures.[5] In particular, the authors claimed that backbones could be not only confined between the mesogenic layers, but also centered in a reduced part of the middle of the layers. In this work, we observed that, going from 55% of mesogens on the backbone to 30%, the ratio of backbone confined in the middle part of the layers significantly increases. Actually, from 55% to 30% of mesogens in the polymer, the ratio liquid crystal to polymer decreases and the backbone can not only be segregated between the layers certainly because of entropic factors. It is even surprising that the material keeps its liquid crystalline properties. Nevertheless, we showed in a previous paper[8] that the thermodynamical

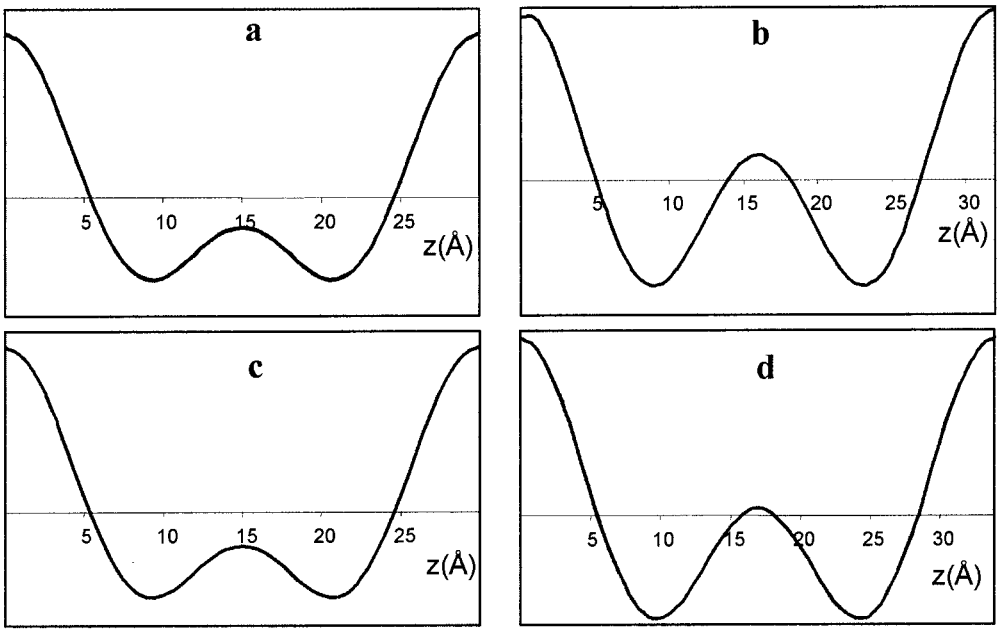

Figure 4. Profiles deduced in the smectic C phases along the normal to the layer (Oz axis) of the distribution of the backbone for polymers $P_{10,6,6}$ 55% (a), $P_{10,6,6}$ 30% (b), $P_{11,8,8}$ 55% (c), and $P_{11,8,8}$ 30% (d). The zero intensity of the main-chain distribution is on the Oz axis.

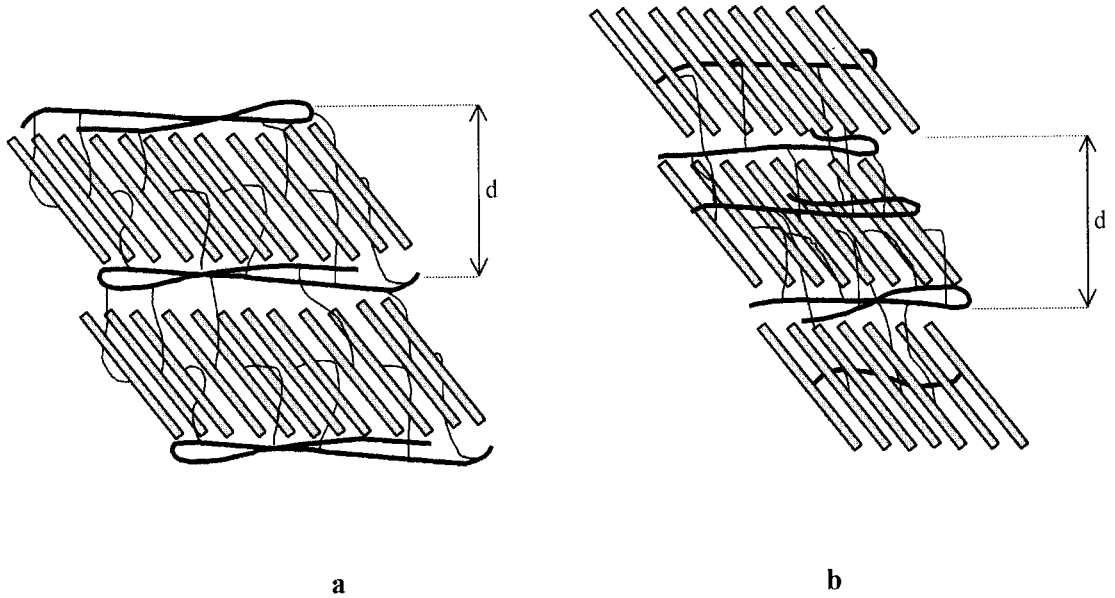

Figure 5. Schematic representation of the model proposed for the distribution of the main chains in the mesogenic layers for polymers with 55% of mesogens (a) and 30% of mesogens (b). *d* represents the layer spacing.

and structural evolution displayed an original behavior as a function of the "dilution". The results obtained on the backbone conformation in the smectic phase also evidence the presence of two regimes in the properties of the materials as a function of the "dilution". The first regime (high percentage of mesogenic side groups) could be driven by strong mesogen−mesogen interactions in the smectic arrangement, resulting from a strong segregation of the polymer backbone between the layers. The driven forces in the second regime (low percentage of mesogenic side groups) are certainly due to the diminution of the mesogenic interactions coupled to the increase of the local flexibility of the backbone. As a result, the micro-organization in the smectic sublayers is different in the regimes as schematically described in Figure 5.

The scheme proposed assumes that the lengths of the spacer and the rod part of the mesogens are slightly the same. As indicated in Figure 1 and ref 2b, such an arrangement is allowed by the symmetry of the system since spacer and hard core are about 20 Å. Moreover, this molecular structure favors the interactions between alkyl parts (and reciprocally between hard cores). The layer is consequently divided in two sublayers in which the proportion of parallel alkyl chains (or parallel rods), is locally higher.

IV. Conclusions

This paper described the evolution of the main-chain conformation and the microsctucture organization in two LCPs with different content of mesogenic groups (55% and 30%). These two "dilutions" have been chosen

to be below and above the optimal content X_{opt} described in another paper.[6] First, a reversible inversion of the conformation from prolate in the nematic phase to oblate in the smectic phase has been described. Moreover, even if the anisotropy ratio ($R_{\parallel}/R_{\perp}$) is small in the nematic phase, it becomes opposite and larger in the smectic phase. This traduces a confinement of the polymer backbone between the layers as observed in other studies.[5,10,11] Nevertheless, we claim that backbones can not only be confined on both sides of the mesogenic layers but also centered in the middle part of the smectic organization. This double layer packing has been described to develop with the "dilution", e.g. when the mesogenic content decreases in the polymer whereas the layer thickness increases. This result is certainly related to the high flexibility of the polysiloxane main chain and the important length of the spacer ($n = 10$ or 11) which authorizes this packing. Moreover, this increase in the layer distance has always been accounted as the result of a swelling of a sublayer containing the polysiloxane backbone in a microphase separation model.[8,12] Nevertheless, this paper evidences that for important "dilution", the phase separation also occurs in the middle part of the mesogenic layers. As described in a previous paper,[6] this system seems to have two regimes, one driven by the mesogens and the other one driven by the polymer. Finally, these materials, with their high anisotropy and their reversible conformation, could certainly find applications in optic, electrooptic, or nonlinear optic devices.

References and Notes

(1) (a) Hessel, F.; Finkelmann, H. *Polym. Bull.* **1985**, *14*, 375. (b) Hessel, F.; Herr, R.; Finkelmann, H. *Makromol. Chem.* **1987**, *188*, 1597. (c) Hessel, F.; Finkelmann, H. *Makromol. Chem.* **1988**, *189*, 2275. (d) Zhou, Q.-F.; Li, H.-M.; Feng, X.-D. *Macromol.* **1987**, *20*, 233. (e) Zhou, Q.-F.; Li, H.-M.; Feng, X.-D. *Mol. Cryst. Liq. Cryst.* **1988**, *155*, 73. (f) Keller, P.; Hardouin, F.; Mauzac, M.; Achard, M. F. *Mol. Cryst. Liq. Cryst.* **1988**, *155*, 171. (g) Gray, G. W.; Hill, J. S.; Lacey, D. *Angew. Chem., Int. Ed. Engl.: Adv. Mater.* **1989**, *28*, 1120. (h) Hardouin, F.; Méry, S.; Achard, M. F.; Mauzac, M.; Davidson, P. *Liq. Cryst.* **1990**, *8*, 565. (i) Lewthwaite, R. W.; Gray, G. W.; Toyne, K. J. *J. Mater. Chem.* **1992**, *2*, 119. (j) Percec, V.; Tomazos, D. *J. Mater. Chem.* **1993**, *3*, 643. (k) Pugh, C.; Schrock, R. *Macromolecules* **1992**, *25*, 6593.

(2) (a) Leube, H. F.; Finkelmann, H. *Makromol. Chem.* **1991**, *192*, 1314. (b) Achard, M. F.; Lecommandoux, S.; Hardouin, F. *Liq. Cryst.* **1995**, *19*, 581. (c) Pugh, C.; Liu, H.; Arehart, S. V.; Narayanan, R. *Macromol. Symp.* **1995**, *98*, 293. (d) Takenaka, S.; Yamasaki, K. *Mol. Cryst. Liq. Cryst.* **1995**, *258*, 51.

(3) (a) Renz, W.; Warner, M. *Phys. Rev. Lett.* **1956**, *56*, 1268. (b) Rieger, J. *Mol. Cryst. Liq. Cryst.* **1988**, *155*, 253. (c) Riegler, J. *J. Phys. Fr.* **1988**, *49*, 253.

(4) (a) Kirste, R. G.; Ohm, H. G. *Makromol. Chem. Rapid. Comm.* **1985**, *6*, 179. (b) Davidson, P.; Keller, P.; Levelut, A. M. *J. Phys.* **1985**, *46*, 939. (c) Keller, P.; Carvalho, B.; Cotton, J. P.; Lambert, M.; Moussa, F.; Pépy, G. *J. Phys. Lett.* **1985**, *46*, 1065. (d) Noirez, L.; Davidson, P.; Schwarz, W.; Pépy, G. *Liq. Cryst.* **1994**, *16*, 1081.

(5) Noirez, L. *Europhysics Lett.* **1998**, *46*, 728.

(6) Lecommandoux, S.; Noirez, L.; Achard, M. F.; Hardouin, F. *J. Phys. II Fr.* **1997**, *7*, 1417.

(7) See for example: (a) Finkelmann, H.; Rehage, G. *Advances in Polymer Science, 60−61*; Springer-Verlag: Berlin, 1984; p 99. (b) Shibaev V. P.; Platé N. A. *Advances in Polymer Science 60-61*; Springer-Verlag: Berlin, 1984; p 175. (c) Mc Ardle, X. *Side chain Liquid Crystal Polymers*; Blackie, Chapman and Hall: New York, 1989.

(8) Lecommandoux, S.; Achard, M. F.; Hardouin, F. *Liq. Cryst.* **1998**, *25*, 85.

(9) Ohm, M. G.; Kirste, R. G.; Oberthür, R. C. *Makromol. Chem.* **1988**, *116*, 1387.

(10) Noirez, L. *Mol. Cryst. Liq. Cryst.* **1995**, *261*, 525.

(11) Cotton, J. P.; Hardouin, F. *Prog. Polym. Sci.* **1997**, *22*, 795.

(12) Diele, S.; Oelsner, S.; Kischel, F.; Ringsdorf, H.; Zentel, R. *Makromol. Chem.* **1987**, *1888*, 1993.

MA9911086